

This is the accepted manuscript made available via CHORUS. The article has been published as:

## Extended tests of an $SU(3)$ partial dynamical symmetry

A. Couture, R. F. Casten, and R. B. Cakirli

Phys. Rev. C **91**, 014312 — Published 16 January 2015

DOI: [10.1103/PhysRevC.91.014312](https://doi.org/10.1103/PhysRevC.91.014312)

# Extended tests of an SU(3)-Partial Dynamical Symmetry

A. Couture\*

*Los Alamos National Laboratory, Los Alamos, New Mexico, 87545, USA*

R. F. Casten

*Wright Nuclear Structure Laboratory, Yale University, New Haven, Connecticut 06520-8124, USA*

R. B. Cakirli

*Department of Physics, University of Istanbul, 34134 Istanbul, Turkey*

**Background:** A recent survey of well-deformed rare earth nuclei showed that B(E2) values from the gamma band to the ground band could be explained rather well by a parameter-free description in terms of a Partial Dynamical Symmetry (PDS).

**Purpose:** Our purpose here is to extend this study to deformed and transitional nuclei in the actinide and  $A \sim 100$  regions to determine if the success of the PDS description is general in medium and heavy mass nuclei and to investigate further where it breaks down.

**Method:** As with the previous study we study the empirical relative B(E2:  $\gamma$  to ground) values in comparison to a pure rotor (Alaga) model and to the SU(3) PDS.

**Results:** The data for the actinides, albeit sparser than in the rare earth region, are reasonably well accounted for by the PDS but with systematic discrepancies. For the Mo isotopes, the PDS improves on the Alaga rules but largely fails to account for the data.

**Conclusions:** As in the rare earths, the parameter-free PDS gives improved predictions compared to the Alaga rules for the actinides. The differences between the PDS predictions and the data are shown to point directly to specific mixing effects. In the Mo isotopes, their transitional character is directly seen in the large deviations of the B(E2) values from the PDS in the direction of the selection rules of the vibrator.

## I. INTRODUCTION

Deformed nuclei have traditionally been described in terms of collective models and the numerical diagonalization of model Hamiltonians. One of the most successful of these, for medium and heavy mass nuclei, has been the Interacting Boson Approximation (IBA) model [1], which is a large truncation of the shell model couched in a group theoretical framework. In the latter perspective the model contains three dynamical symmetries, that is, the Hamiltonian can be written in terms of a group called U(6) and its subgroups. These symmetries can be solved analytically and allow the states to be labeled by many-body quantum numbers. This leads to specific selection rules and analytic predictions for many observables.

One of these three dynamical symmetries is SU(3) which describes a particular type of deformed rotor nucleus with low lying  $K = 2$  ( $\gamma$ ) and  $K = 0$  (often called  $\beta$ ) excitation modes along with rotational bands built upon them in which levels of the same spin in the two bands are degenerate. In this limit transitions from the  $\gamma$  band to the ground band are forbidden. Empirically, these bands are seldom degenerate and  $\gamma$  to ground band B(E2) values are known to be collective (typically 5-10 W.u.). Clearly these two features would seem to rule out an SU(3) description: not surprisingly, most collective model descriptions of these nuclei have used broken-

SU(3) numerical diagonalizations of the IBA Hamiltonian.

However, Leviatan proposed [2] that the idea of Partial Dynamical Symmetry (PDS) could account for the low energy data on deformed nuclei. The idea of the PDS is that the ground and  $\gamma$  bands retained pure SU(3) symmetry but that all other states exhibited broken symmetry. This symmetry breaking allows one to account for the  $\gamma - \beta$  degeneracy-breaking. Collective  $\gamma$  to ground band B(E2) values were obtained by generalizing the E2 operator in the IBA. As explained in Ref. [3] (see discussion around Eq. 1 in that reference) this has the special feature that relative  $\gamma$  band to ground band B(E2) values are parameter free.

Leviatan presented evidence for the success of the SU(3)-PDS in the data for  $^{168}\text{Er}$ . The question naturally arose as to whether this was accidental or whether the PDS was generally applicable to deformed nuclei. Very recently, we published [3] the first extensive study of this PDS which surveyed a wide range of rare earth nuclei from Sm to Os. It was found that the PDS provides a reasonably good description of extensive data on these nuclei but that discrepancies remained and were systematic. It was shown that the PDS directly incorporates finite valence nucleon number ( $N_{\text{val}}$ ) facets of structure and that deviations of the PDS from the data could be specifically ascribed to the need for further symmetry breaking (mixing of low lying bands) that could be accomplished numerically with IBA calculations.

In addition to the evidence for the realization of an SU(3) PDS in the deformed rare earth nuclei, recent work

---

\* Corresponding Author: acouture@lanl.gov

[4–6] has found evidence for other PDS or Quasi Dynamical Symmetries (QDS). These results, taken together, lead to the realization that symmetry behavior is not limited to the vertices of the IBA symmetry triangle. Instead, the interior of the triangle has abundant remnants of the dynamical symmetries such as an  $O(6)$ -based PDS and the arc of regularity which is an  $SU(3)$ -based QDS. Since symmetries reflect regular spectra, this alters our understanding of the roles of order and chaos throughout the triangle. Further, it offers a potentially new perspective on collective behavior in medium and heavy mass nuclei and the possibility of an enhanced role for symmetry-based analytic solutions, quantum numbers, and specific selection rules.

It is the purpose of the present study to extend the work of Ref. [3] to other mass regions, notably the  $A \sim 100$  and actinide regions, to investigate whether a PDS description is also valid beyond the rare earth region.

## II. METHODS

The essential PDS predictions are the  $\gamma - \beta$  band degeneracy breaking and the  $\gamma$  band to ground band interband relative  $B(E2)$  values. The former can always be fit since the PDS Hamiltonian has two adjustable parameters. But the relative  $B(E2)$  values are independent of that parameter choice, parameter-free, and therefore they are robust predictions of the PDS. In Ref. [3] it was found, for the rare earth region, that the PDS gives significantly better agreement with the data for these  $B(E2)$  values than the Alaga rules [7], that the PDS predictions depend only on  $N_{\text{val}}$ , and that existing numerical IBA calculations, such as the CQF calculations of Refs. [8, 9] provide improved agreement because they include the mixing of  $SU(3)$  representations.

For the present study we assembled all available data on deformed actinide nuclei as well as on the transitional Zr-Mo isotopes (to probe a very different kind of region) from the Nuclear Data Sheets (NDS) [10]. Where unevaluated (“XUNDL”) data exist and are relevant, we make note of that as well.

Both the actinide and the Zr-Mo region data are far less extensive and accurate than in the rare earth region. Nevertheless, sufficient data exist to carry out useful comparisons and to extract meaningful conclusions. Having surveyed the data, we note that  $E2/M1$  mixing ratios ( $\delta$  values) are virtually non-existent in both mass regions, that some transitions that one would expect to be  $E2$  are listed as  $M1$  in the NDS, and that most of the data (especially in the actinides) stem from older work, typically in the 1970’s, carried out with one or two rather small Ge or Ge(Li) detectors. There is clearly a strong motivation for new studies, usually  $\beta$  decay, with modern clover detectors that would have substantial nuclear structure impact.

## III. RESULTS

The results are summarized in Table I for the actinides and Table II for Mo (there are no usable data for Zr) in comparison with the Alaga rules, the PDS predictions, and, in Table I, the data for the benchmark nucleus  $^{168}\text{Er}$ . We have noted that the PDS predictions deviate from the Alaga rules solely due to finite valence nucleon number effects. Therefore, naturally, they are valence-nucleon-number-dependent. However, as seen in Table I, this dependence is rather weak for valence nucleon numbers typical of deformed nuclei (compared to the differences between the data and the Alaga rules), and hence it is sufficient in Table I to bracket the data by the PDS predictions for the lowest ( $N_{\text{val}}=20$ ) and highest ( $N_{\text{val}}=32$ ) valence nucleon numbers. In Table I  $N_{\text{val}}$  increases from left to right, and, not surprisingly, so does  $R_{4/2}$ , from transitional values in the lighter actinides, to well-developed rotational behavior starting at  $A \sim 234$ . For the Mo isotopes in Table II, there are three adjacent even-even nuclei with sufficient data and hence we show the PDS predictions for the central valence nucleon number.

The Tables show a number of interesting results. First we note that in Table I, the value 480 for the  $4_{\gamma}^{+} \rightarrow 6_{\gamma}^{+}$  transition in  $^{240}\text{Pu}$  is more than an order of magnitude larger than the corresponding transitions in  $^{168}\text{Er}$  and in most of the rare earth nuclei—and beyond the scope of any existing model. We find no obvious error in the data, but, clearly, it should be re-measured. We have ignored this value in the discussion below.

Turning now to Table I, we note the same general patterns as in the rare earth region [3]. Namely, spin-decreasing transitions are nearly always less than the Alaga rules, and spin-increasing transitions are nearly always greater than the Alaga rules. The main exceptions are the  $2_{\gamma}^{+} \rightarrow 4_{\gamma}^{+}$  transition in  $^{228}\text{Th}$ , the  $3_{\gamma}^{+} \rightarrow 4_{\gamma}^{+}$  transition in  $^{236}\text{U}$ , and the  $4_{\gamma}^{+} \rightarrow 6_{\gamma}^{+}$  transitions in  $^{228}\text{Th}$  and  $^{234}\text{U}$ .

Figure 1 gives a clearer perspective on the data and trends for the spin decreasing transitions  $2_{\gamma}^{+} \rightarrow 0_{\gamma}^{+}$ ,  $4_{\gamma}^{+} \rightarrow 2_{\gamma}^{+}$ , and  $6_{\gamma}^{+} \rightarrow 4_{\gamma}^{+}$  for all the isotopes considered here. The PDS predictions for  $N_{\text{val}}=20$  and  $N_{\text{val}}=32$  are on the left and right, bracketing the values applicable to these nuclei. The Alaga rules and the results from Ref. [3] for  $^{168}\text{Er}$  are shown on the right. In all cases the data are below the Alaga rules. The PDS predictions include the effects of  $N_{\text{val}}$ . Hence they differ from the Alaga rules and are closer to the data. This is an important conclusion as it further establishes the  $SU(3)$  PDS as an important refinement of the rotational model because it includes consequences of the fact that the nucleus is a finite system. Nevertheless, the PDS still over-predicts the data. As discussed in Ref. [3], this suggests the need for mixing of  $SU(3)$  representations.

The trend from top to bottom in Figure 1 is particularly informative regarding such mixing. We see that

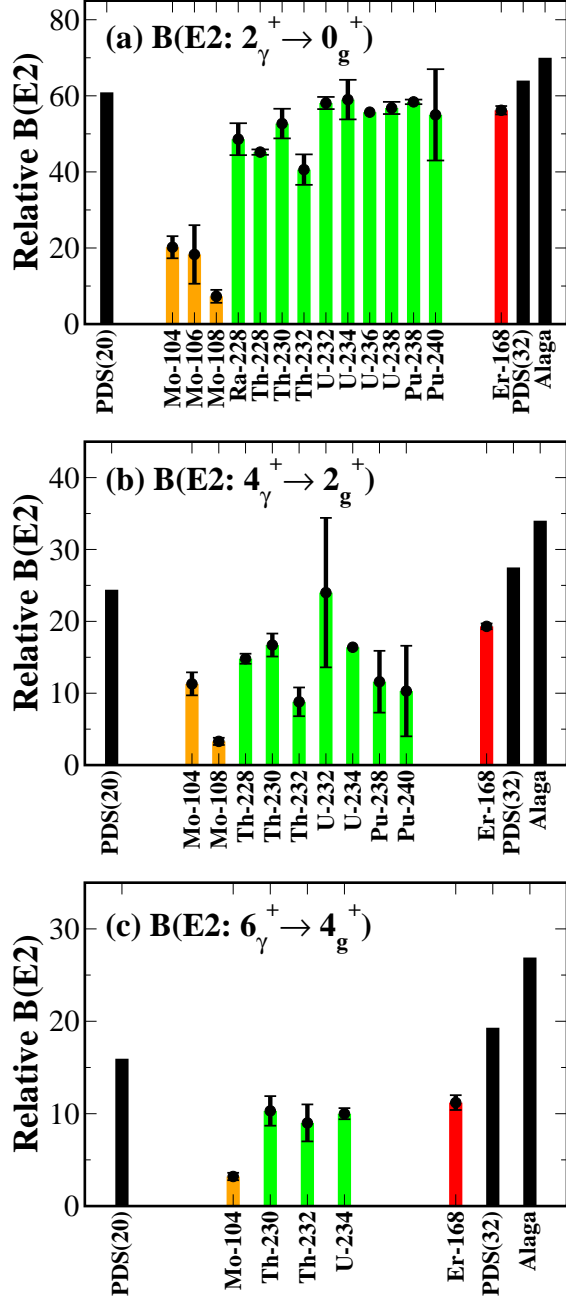


FIG. 1. (Color online) Shown above are relative  $B(E2)$  transition strengths for  $2_{\gamma}^{+} \rightarrow 0_{g}^{+}$  (panel a/top),  $4_{\gamma}^{+} \rightarrow 2_{g}^{+}$  (panel b/middle), and  $6_{\gamma}^{+} \rightarrow 4_{g}^{+}$  (panel c/bottom) transitions. As in the tables, all transition strengths are normalized to the strongest Alaga transition ( $J_{\gamma}^{+} \rightarrow J_{g}^{+}$  for these cases). Error bars are shown for nuclei with reported uncertainties in NDS [10]. For visual clarity,  $^{106}\text{Mo}$  has been omitted from the  $4_{\gamma}^{+} \rightarrow 2_{g}^{+}$  plot as the error bars were greater than 50%, severely limiting the information it provides. Plotted with the Mo and actinide data are  $^{168}\text{Er}$  for reference, the PDS for  $N_{\text{val}}=20$  and  $N_{\text{val}}=32$ , and the Alaga rules.

the actinide data are increasingly lower as the spin of the initial gamma band state increases. For the  $2_{\gamma}^{+} \rightarrow 0_{g}^{+}$  transitions, the data are, on average, about 80% of the Alaga rules. For the  $4_{\gamma}^{+} \rightarrow 2_{g}^{+}$  transitions, the data are about 50% of the Alaga rules. For the  $6_{\gamma}^{+} \rightarrow 4_{g}^{+}$  transitions, the data are about 40% of the Alaga rules. A similar trend applies in comparison to the PDS.

In the standard band-mixing scenario, the mixing matrix elements increase roughly as the square of the initial spin. The effect of the mixing is to reduce the relative strengths of the spin-decreasing transitions. Therefore, these transition strengths will become successively smaller as the gamma band spin increases. This is exactly what is seen in Fig. 1. Turning the argument around, the trend in Fig. 1 is very direct evidence that the differences between the PDS and the data are specifically due to band-mixing (mixing of SU(3) representations).

Further support for representation mixing is seen in Table I. Generally, the transitions that increase the spin are stronger than the Alaga rules, and roughly the same or slightly larger than the PDS. In a band mixing scenario, the feature that spin-decreasing and -increasing transitions behave oppositely relative to the Alaga rules is a direct consequence of a consistent sign for the mixing matrix elements as a function of spin [15].

The results for  $^{104-108}\text{Mo}$  are shown in Table II. The Mo data reflect a different situation than in the actinides, namely, nuclei that are far from rotational. Due to the large quasi-rotational spacings in Mo (e.g.,  $E(4_{\gamma}^{+}) \sim 500-600$  keV), the transition energies for spin-increasing transitions (such as  $4_{\gamma}^{+} \rightarrow 6_{g}^{+}$ ) are quite small and hence these transition rates are very strongly hindered by the  $E_{\gamma}^5$  factor connecting measured intensities to relative  $B(E2)$  values. Moreover, they are inherently weak due to the small Clebsch-Gordan coefficients for such transitions (seen in the small Alaga rules) which have a simple origin in the rotational/intrinsic angular momentum composition of the wave functions [3]. Therefore it is not surprising that they have not been found.

With  $R_{4/2}$  values of  $R_{4/2} \sim 3$ , these Mo isotopes are well-centered in the transitional region. As found in Fig. 2 of Ref. [3] for transitional nuclei, although the PDS is an improvement over the Alaga rules for such nuclei, it is far from the data and, not surprisingly, the PDS fails for these Mo isotopes which are very far from any version of SU(3)—pure or partially broken. This is very vividly seen in Fig. 1 where, across the three panels, the relative  $B(E2)$  values in Mo are much smaller than in the actinides,  $^{168}\text{Er}$  (typical of the well-deformed rare earth nuclei), the PDS or the Alaga rules—typically by a factor of 2 or more. Further, the behavior for the spin-decreasing transitions can be rather easily understood in terms of the transitional character of these nuclei. Consider Fig. 2, which shows the states that we have been discussing from the perspective of the vibrator model.

In the vibrator model, the levels are arranged in equally spaced phonon multiplets. Figure 2 shows that the spin-decreasing transitions from non-yrast to yrast

## Vibrator

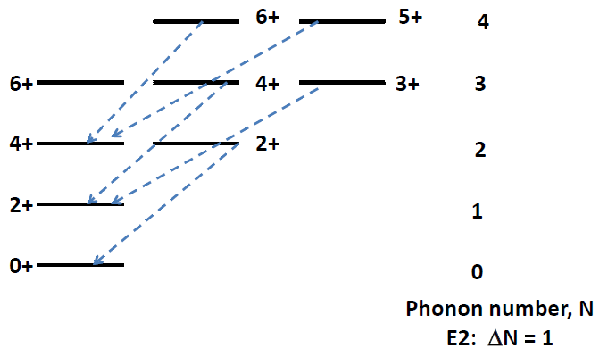


FIG. 2. (Color online) Partial vibrator level scheme showing the phonon structure for the yrast and next lower spin non-yrast levels. The transitions shown as dashed lines in the figure are forbidden in the vibrator since they change the phonon number by 2.

states are forbidden by the vibrator selection rules—they change the phonon number by  $\Delta N = -2$ . Of course, these Mo isotopes, with  $R_{4/2} \sim 3$ , are at least as far from the vibrator as they are from the rotor. Nevertheless, we can inspect the Mo data to see if the deviations from the rotor and the PDS are in the *direction* of the vibrator, that is, that the spin-decreasing transitions become smaller. As seen in Fig. 1, that is exactly the observed trend. Note that this also accounts for the seemingly anomalous value for the  $3_\gamma^+ \rightarrow 4_g^+$  entry for  $^{108}\text{Mo}$  in Table II where we have normalized to the strongly hindered spin decreasing transition. Additional data on the branching ratios from the  $3_\gamma^+$  level in the other Mo isotopes would be valuable.

In retrospect, exactly the same physics can be seen in Ref. [3] for the transitional nuclei in Fig. 2 of that paper, although it was not noticed until now. Those nuclei belong to two categories—transitional between vibrator and rotor ( $^{152}\text{Sm}$ ,  $^{154}\text{Gd}$ ) and transitional between rotor and  $\gamma$ -soft (Os nuclei). However, the latter  $\gamma$ -soft nuclei have the same  $O(5)$  symmetry as the vibrator and therefore exactly the same selection rules for these transitions.

## IV. CONCLUSIONS

We have tested an  $SU(3)$  PDS in the well-deformed actinides and in the transitional Zr-Mo region. In both re-

gions, one conclusion that stands out is the serious need for more, and more accurate, measurements to update existing data that were mostly accumulated decades ago with fewer and less efficient  $\gamma$ -ray detectors. Many weak, usually lower energy, spin-increasing  $\gamma$  band to ground band transitions are absent from the data and many  $E2/M1$  mixing ratios are unknown.

In the actinides, overall, the data are similar to the rare earth region. The PDS is an improvement compared to the Alaga rules. The most telling data are for the spin-decreasing transitions, especially  $2_\gamma^+ \rightarrow 0_g^+$ ,  $4_\gamma^+ \rightarrow 2_g^+$ , and  $6_\gamma^+ \rightarrow 4_g^+$ , which show an interesting and informative trend with spin that has not been noticed before. As the spin,  $J_\gamma$ , of the initial gamma band state increases, the relative interband  $B(E2)$  values become successively smaller relative to the PDS. This is easily seen in Fig. 1. As discussed in Ref. [3], differences with the PDS are suggestive of mixing of  $SU(3)$  representations (band mixing in common usage). Such mixing should increase with spin. Therefore the relative  $B(E2)$  values should fall further and further below the PDS predictions as the gamma band spin increases. The present data (Fig. 1) show exactly this feature, pointing rather directly to mixing of  $SU(3)$  representations as the needed ingredient beyond the PDS. In the Mo isotopes, while the PDS again improves on the Alaga predictions, both the Alaga rules and the PDS results are very far from the data. Specifically, the spin-decreasing transitions (the spin-increasing ones are not known) are quite weak. As these are transitional nuclei, and as these transitions are forbidden in the vibrator limit, this is reasonable. The same feature is seen in the transitional rare earth nuclei although it was not noticed in Ref. [3].

## ACKNOWLEDGMENTS

We are grateful to Klaus Blaum, Ami Leviatan, and Norbert Pietrella for useful discussions.

This material is based upon work supported by the U.S. Department of Energy, Office of Science, Office of Nuclear Physics, under Award Number DE-FG02-91ER40609 and contract number DE-AC52-06NA25396. R.B.C. acknowledges support by the Max-Planck Partner group.

- 
- [1] F. Iachello and A. Arima, *The Interacting Boson Model* (Cambridge University Press, Cambridge, England, 1987).
  - [2] A. Leviatan, Phys. Rev. Lett. **77**, 818 (1996).
  - [3] R. F. Casten, R. B. Cakirli, K. Blaum, and A. Couture, Phys. Rev. Lett. **113**, 112501 (2014).

- [4] P. Van Isacker, Phys. Rev. Lett. **83**, 4269 (1999).
- [5] A. Leviatan and P. V. Isacker, Phys. Rev. Lett. **89**, 222501 (2002).
- [6] C. Kremer, J. Beller, A. Leviatan, N. Pietralla, G. Rainovski, R. Trippel, and P. Van Isacker, Phys. Rev. C **89**, 041302 (2014).

- [7] G. Alaga, K. Alder, A. Bohr, and B. R. Mottelson, Dan. Mat. Fys. Medd. **29**, 1 (1955).
- [8] D. D. Warner and R. F. Casten, Phys. Rev. Lett. **48**, 1385 (1982).
- [9] E. A. McCutchan, N. V. Zamfir, and R. F. Casten, Phys. Rev. C **69**, 064306 (2004).
- [10] “National nuclear data center ENSDF web program,” (2014), <http://www.nndc.bnl.gov/ensdf/>.
- [11] A. Demidov, L. Govor, V. Kurkin, and I. Mikhailov, Physics of Atomic Nuclei **71**, 1839 (2008).
- [12] L. Govor, A. Demidov, V. Kurkin, and I. Mikhailov, Physics of Atomic Nuclei **77**, 131 (2014).
- [13] T. Kotthaus, P. Reiter, B. Bruyneel, M. Chatzistamatiou, J. Eberth, G. Gersch, H. Hess, I. Stefanescu, N. Warr, D. Weisshaar, A. Wiens, T. Morgan, R. Lutter, W. Schwerdtfeger, P. G. Thirolf, P. Bringel, H. Hübel, and A. Neusser-Neffgen, Phys. Rev. C **88**, 064306 (2013).
- [14] A. Guessous, N. Schulz, M. Bentaleb, E. Lubkiewicz, J. L. Durell, C. J. Pearson, W. R. Phillips, J. A. Shannon, W. Urban, B. J. Varley, I. Ahmad, C. J. Lister, L. R. Morss, K. L. Nash, C. W. Williams, and S. Khazrouni, Phys. Rev. C **53**, 1191 (1996).
- [15] L. L. Riedinger, N. R. Johnson, and J. H. Hamilton, Phys. Rev. **179**, 1214 (1969).

TABLE I. Relative B(E2) values for the actinides.<sup>a</sup>

$J_i^\pi \rightarrow J_f^\pi$	PDS	<sup>228</sup> Ra	<sup>228</sup> Th	<sup>230</sup> Th	<sup>232</sup> Th <sup>b</sup>	<sup>232</sup> U	<sup>234</sup> U	<sup>236</sup> U <sup>c</sup>	<sup>238</sup> U <sup>b</sup>	<sup>238</sup> Pu	<sup>240</sup> Pu	<sup>168</sup> Er	PDS	ALAGA
$N_{\text{val}}$	20	20	20	22	24	24	26	28	30	30	32	32	32	
$R_{4/2}$		3.21	3.23	3.23	3.28	3.29	3.30	3.30	3.30	3.31	3.31	3.31		
$2_\gamma^+ \rightarrow 0_g^+$	60.9	48.6 (42)	45.2 (7)	52.7 (39)	40.6 (40)	58.1 (16)	59.0 (52) <sup>d</sup>	55.7	56.8 (16)	58.4 (6)	55 (12)	56.2 (11)	64.0	70
$2_\gamma^+ \rightarrow 2_g^+$	100	100	100	100	100	100	100	100	100	100	100	100	100	100
$2_\gamma^+ \rightarrow 4_g^+$	6.9		4.0 (2)	7 (3)		5.7 (2)	5.6 (7)		6.2 (4)	5.6 (1)		7.3 (4)	6.2	5
$3_\gamma^+ \rightarrow 2_g^+$	100	100	100	100	100	100	100	100		100	100	100	100	100
$3_\gamma^+ \rightarrow 4_g^+$	55.6	53.2 (42)	68.3 (24)	62 (10)	55 (13)	55.0 (45)	42.5 (55)	23.2		50.6 (8)	52 (7)	62.6 (14)	49.3	40
$4_\gamma^+ \rightarrow 2_g^+$	24.4		14.8 (7)	16.7 (16)	9 (2)	24 (10)	16.4			11.6 (43)	10 (6)	19.3 (4)	27.5	34
$4_\gamma^+ \rightarrow 4_g^+$	100		100	100	100	100	100			100	100	100	100	100
$4_\gamma^+ \rightarrow 6_g^+$	14.6		6.3 (14)	28 (7)	19 (6)		4.7 (4)				480 (130)	13.1 (12)	12.0	8.64
$5_\gamma^+ \rightarrow 4_g^+$	100			100	100		100	100				100	100	100
$5_\gamma^+ \rightarrow 6_g^+$	96.4			184 (18)	174 (19)		98.7					123 (14)	79.6	57.1
$6_\gamma^+ \rightarrow 4_g^+$	16.0			10.3 (16)	9 (2)		10.0 (6)					11.2 (10)	19.3	26.9
$6_\gamma^+ \rightarrow 6_g^+$	100			100	100		100					100	100	100
$6_\gamma^+ \rightarrow 8_g^+$	21.9						14.7 (15)					37.6 (72)	16.7	10.6

<sup>a</sup> E2/M1 mixing corrections and their uncertainties have been included where  $\delta$ -values were reported in NDS. If no  $\delta$ -values were reported, transitions were assumed to be pure E2.

<sup>b</sup> Additional branching ratios are reported in XUNDL from Refs. [11, 12], but these measurements report on  $^{232}\text{Th}(n, n')$  and  $^{238}\text{U}(n, n')$  experiments performed with a single 20% HPGe detector. While there were some additional transitions reported, others differed from the NDS values, and there were complications in disentangling the  $^{232}\text{Th}$  and  $^{238}\text{U}$  decays from fission products. Those results are not reflected here.

<sup>c</sup> No uncertainties were reported on the  $\gamma$ -ray intensities in the NDS for this nucleus.

<sup>d</sup> A relative B(E2) value of 74 with no uncertainty is reported by Ref. [13] for this transition. This value is larger than the Alaga rules, which is inconsistent with the other results.

TABLE II. Relative B(E2) values for the Mo isotopes.<sup>a</sup>

$J_i^\pi \rightarrow J_f^\pi$ $N_{\text{val}}$ $R_{4/2}$	Alaga	PDS	<sup>104</sup> Mo	<sup>106</sup> Mo	<sup>108</sup> Mo
		22	20	22	24
			2.92	3.05	2.92
$2_\gamma^+ \rightarrow 0_g^+$	70.0	61.6	20.2 (29)	18 (8)	7.3 (17)
$2_\gamma^+ \rightarrow 2_g^+$	100	100	100	100	100
$3_\gamma^+ \rightarrow 2_g^+$	100	100.0			100
$3_\gamma^+ \rightarrow 4_g^+$	40.0	54.0			1270 (190)
$4_\gamma^+ \rightarrow 2_g^+$	34.0	25.1	11.3 (16) <sup>b</sup>	13 (9)	3.3 (5)
$4_\gamma^+ \rightarrow 4_g^+$	100	100	100	100	100
$6_\gamma^+ \rightarrow 4_g^+$	26.9	16.7	3.2 (4)		
$6_\gamma^+ \rightarrow 6_g^+$	100	100	100		

<sup>a</sup> No  $\delta$ -values were reported in NDS, so all transitions were assumed to be pure E2.

<sup>b</sup> An alternate relative B(E2) value of 5.7 (13) is reported in NDS from Ref. [14].